ISSN 0023-1584, Kinetics and Catalysis, 2015, Vol. 56, No. 4, pp. 419–427. © Pleiades Publishing, Ltd., 2015.

Kinetic Study of Esterification of Acetic Acid with Methanol over Indion 190 Acidic Solid Catalyst[1]

Mekala Mallaiah* and Goli Venkat Reddy

Department of Chemical Engineering, National Institute of Technology, Warangal 506004, India

**e-mail: mmyadav2001@gmail.com*

Received August 27, 2014

Abstract—Esterification of acetic acid with methanol to synthesize methyl acetate in an isothermal well-mixed batch reactor was studied in the temperature range of 323.15–353.15 K. Indion 190 ion-exchange resin was used as a solid catalyst. Feed molar ratios were varied from 1 : 1 to 1 : 4. The influence of temperature, catalyst loading, stirring rate, catalyst particle size and initial molar ratio on the reaction rate was investigated. Experimental results showed that the reaction is kinetically controlled. The sorption experiments were carried out independently to find the adsorption constants. For the constituent components the values of adsorption constants decrease in the order of water > methanol > acetic acid > methyl acetate. The kinetic data were correlated with the pseudo-homogeneous (ideal and non-ideal), Eley–Rideal and Langmuir–Hinshelwood–Hougen–Watson (LHHW) models to determine the kinetic parameters. All the models were suitable to predict the experimental data, but with the LHHW model a more accurate match of the experimental data was achieved.

Keywords: kinetics, esterification, Indion 190 catalyst, adsorption, non-ideal model, LHHW model

DOI: 10.1134/S0023158415040126

INTRODUCTION

Organic esters are very important chemicals. There is a wide range of applications of organic esters such as production of cosmetics, plasticizers, pharmaceutical substances, polymers, textiles, flavours and in food industry. Several synthetic processes are available to obtain organic esters. A comprehensive review of esters synthesis is available [1]. Methyl acetate manufactured commercially is in great demand. It is especially useful for the manufacturing nail polish removers, printing inks, perfumery, paints, dyes, industrial coatings and as a solvent in adhesives.

Methyl acetate is produced by the esterification reaction between the acetic acid and methanol. At room temperature, the reaction is very slow and reversible and several days are usually required to attain equilibrium in the absence of the catalyst. The addition of the catalyst increases the reaction rate and therefore decreases the time needed to reach an equilibrium state. One can discriminate between heterogeneous and homogeneous catalytic reactions. Homogenous catalysis occurs when the catalyst and the reactants are both in the same phase while in the case of heterogeneous catalysis the catalyst and the reactants are in different phases. Homogeneous catalysts, such as HCl, HI, H_2SO_4, and HBr, provide an acid medium. Ion-exchange resins are frequently used as heterogeneous catalysts. Heterogeneous catalysts are preferable to the homogeneous catalysts due to several advantages like easy separation of catalyst from the post reaction mixture, better selectivity towards desired product, high purity of the product due to suppression of side reactions and elimination of the corrosive environment [2].

One of the earliest works relating to kinetics of catalytic esterification of acetic acid with methanol was published by Rolfe and Hinshelwood [3]. Ronnback et al. [4] investigated the kinetics of esterification of acetic acid with methanol using a homogeneous hydrogen iodide as a catalyst. It was observed that hydrogen iodide also reacted with methanol and produced methyl iodide as a by-product. Agreda et al. [5] proposed a rate expression for the esterification reaction in which sulphuric acid was used as a homogeneous catalyst.

Many solid catalysts were used, such as solid acids and bases, ion-exchange resins, zeolites and acid clay catalysts. Ion-exchange resins are the most common heterogeneous catalysts used for esterification reaction [6–8]. These ion-exchange resins not only catalyse the reaction but also improve conversion because of selective adsorption of reactants and swelling nature [9, 10]. In the heterogeneous catalysis, the active solid surface can distort or even dissociate an absorbed reactant molecule and increase the rate of reaction [11].

Most of the esterification reactions were studied by using the solid catalyst Amberlyst 15 [12–18]. Liu et al. [19] investigated the similarities and differences between heterogeneous and homogeneous catalysed

[1] The article is published in the original.

Table 1. Physico-chemical properties of Indion 190 catalyst

Physical property	Indion 190
Manufacturer	"Ion Exchange India Ltd."
Shape	Beads
Physical form	Opaque, faint dark grey coloured
Size, μm	725
Apparent bulk density, g/cm^3	0.55–0.60
Surface area, m^2/g	28–32
Pore volume, mL/g	0.32–0.38
Operating temperature T_{max}, °C	150
Hydrogen ion capacity, meq/g	4.7
Matrix type	Styrene–DVB
pH range	0–7
Resin type	Macroporous strong acid cation
Functional group	SO_3^-
Ionic form	H^+

esterifications. They studied the kinetics of acetic acid esterification with methanol using a commercial Nafion/silica nano composite catalyst (SAC-13) and H_2SO_4. The kinetic behaviour of esterification of acetic acid with methanol was investigated by Tsai et al. [20], who used Amberlyst 36 as a solid catalyst in a packed-bed reactor in the temperature range of 313.15–328.15 K with the molar ratio of methanol to acetic acid varied from 1 to 5.

In the present work, esterification of acetic acid with methanol was studied in the presence of the solid acid catalyst Indion 190. This catalyst has received little attention. For the first time adsorption of acetic acid, methanol, methyl acetate, and water on Indion 190 catalyst surface from binary mixtures was conducted. For the first time the swelling of Indion 190 catalyst in the presence of acetic acid, methanol, methyl acetate and water could be described. Moreover, in the present study ideal and non-ideal based kinetic models were used to correlate the experimental data. The effect of various parameters like stirring rate, size of catalyst particle, reaction temperature, reaction time, catalyst loading and initial reactant concentration on the esterification was studied. Four types of kinetic models, pseudo-homogeneous (ideal and non-ideal), Eley-Rideal (ER) and Langmuir-Hinshelwood-Hougen-Watson (LHHW) models were evaluated and the best kinetic model was proposed for the esterification reaction.

EXPERIMENTAL

Chemicals

Methanol (purity of 99 wt %) and acetic acid (purity of 99.95 wt %), supplied by SD Fine Chemicals Ltd. (India), were used in the present study.

Catalyst

The solid acid catalyst, Indion 190, used for the esterification reaction was supplied by Ion-Exchange India Ltd. Indion 190 has cross-linked three-dimensional structures of polymeric material, obtained by sulfonation of a copolymer of polystyrene and divinyl benzene (DVB). It is an opaque and faint dark grey coloured solid spherical bead. The ion-exchange resin was dried for 2 h in an air oven at temperature 363.15 K to remove the moisture. The physicochemical properties of the solid ion-exchange resin catalyst are shown in Table 1.

Experimental Setup

The esterification reaction was carried out in a 500 mL three neck round-bottom flask. The flask was placed in a heating rota mantle, which contained a heating knob, stirrer and a speed control knob. The rotational speed of magnetic stirrer was varied from 240 to 640 rpm, using the speed control knob. A spiral condenser was connected to the reaction flask vertically to condense the vapours and mix them back with the reacting mixture. A mercury thermometer was inserted into the flask to measure the temperature of the reaction mixture. The accuracy of the thermometer is within ±0.5 K.

Experimental Procedure

The reactants were weighed using a digital electronic balance with an accuracy of ±0.0001 g. In the experiment, equimolar quantities of methanol (32 g) and acetic acid (60 g) were mixed and charged to the reactor. The reaction mixture was heated and when it reached the desired temperature, the catalyst was added to the mixture and the time was noted ($t = 0$). The temperature was measured by mercury thermometer within an error of ±0.5 K. Samples of the reaction mixture were withdrawn at regular intervals of time. The samples were placed in a refrigerator prior to analysis, to prevent further reaction. The reaction mixture was analyzed by Gas chromatography (GC) for components of the mixture.

The following reaction takes place in the reacting mixture.

$$CH_3COOH\ (\mathbf{A}) + CH_3OH\ (\mathbf{B}) \rightleftharpoons CH_3COOCH_3\ (\mathbf{C}) + H_2O\ (\mathbf{D}).$$

Water is also formed along with methyl acetate.

Sorption Equilibrium and Swelling Experiments

The sorption experiments were carried out for 4 nonreactive binary mixtures at a constant temperature of 298.15 K. The nonreactive mixtures studied were: water-methanol, water-acetic acid, methyl acetate-methanol, and methyl acetate-acetic acid. These experiments were carried out according to the procedure proposed by Popken et al. [12]. The binary sample of known quantity (a total of 10 g) was mixed with the known quantity of catalyst (1.0 g) in 20 mL glass vials. After reaching an equilibrium state in about 2–3 weeks, the samples were analysed using gas chromatography. The difference between the initial and final quantity of binary mixture in the vial was taken as the quantity of adsorbed material.

To find out the swelling nature of the catalyst in the presence of pure components like methanol, acetic acid, methyl acetate and water, experiments were conducted at a constant temperature of 298.15 K in sealed graduated cylinder of volume of 20 mL. A known amount of dry catalyst (1.0 g) of known particle diameter was placed in the glass cylinder followed by adding a pure component. The experiments were carried out for each component separately. The solid catalyst and the pure component were allowed to remain in contact with each for about 2–3 weeks, till equilibrium was reached. After 2 weeks, the samples were withdrawn from the cylinder and the diameter of the catalyst particle was measured using an optical microscope. The particle size was measured after every 2 days, thereafter. If there was no change in the size of the catalyst particle between 2 successive measurements, then it was considered as the system had reached an equilibrium state. When the system attained equilibrium, the diameter of the catalyst particle was measured and the swelling ratio was calculated.

Analysis

The samples were analyzed using a GC-2014 ATF gas chromatograph (“Schimadzu”, Japan) equipped with a thermal conductivity detector. Porapak-Q (2 m length and 3.17 mm i.d.) packed column was used to analyze the sample. High purity hydrogen gas was used as a carrier gas at a flow rate of 30 mL/min. The oven temperature was programmed at 323.15 K for 1 min and then raised from an initial value of 323.15 to 443.15 K at a ramp rate of 10 K/min and was held at 443.15 K for 2 min. The detector temperature was maintained at 473.15 K.

EXPERIMENTAL RESULTS

Esterification reaction with Indion 190 ion-exchange resin catalyst was investigated at (1 : 1) molar ratio of acetic acid to methanol. The temperature was varied from 323.15 to 353.15 K. The catalyst concentration based on initial reaction mixture was varied from 0.01 to 0.05 g/mL. The stirring rate was varied from 240 to 640 rpm and the average catalyst particle size was varied from 425 to 925 μm. The effect of different parameters on reaction kinetics is discussed below.

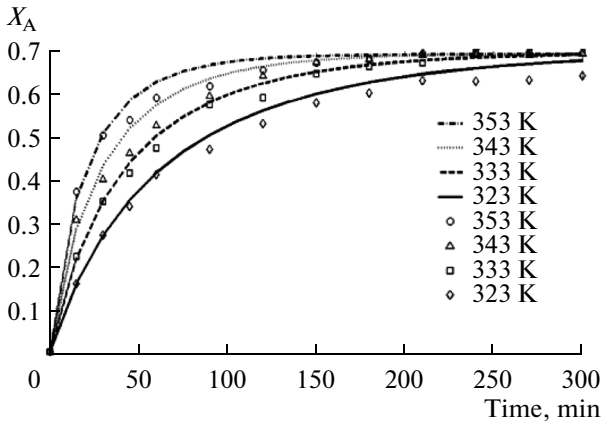

Fig. 1. Conversion of acetic acid for different temperatures. [Catalyst] = 0.025 g/mL. Dashed lines represent the LHHW model predictions.

Effect of Reaction Temperature

The experimental data obtained at different temperatures with the fixed catalyst concentration of 0.025 g/mL along with the predictions obtained from LHHW model is shown in Fig. 1. From the plot, it could be observed that the conversion of acetic acid increases with temperature. This indicates that the reaction rate is controlled by temperature. The higher the temperature the less the time needed for the system to reach equilibrium.

Effect of Catalyst Loading

Experiments were conducted with different catalyst concentrations in the range of 0.01 to 0.05 g/mL. The experimental results obtained with different catalyst concentrations at 343.15 K are shown in Fig. 2 along with the expected values derived from the LHHW model. Figure 2 indicates that as the catalyst loading increases both the conversion of acetic acid and the reaction rate increase. The increase in reaction rate with the catalyst loading can be explained by the increased availability of H^+ ions. This behaviour can be verified by calculating the initial rate of reaction at different catalyst concentrations. The initial rate of reaction is calculated by

$$-r_{A0} = \frac{n_{A0}}{W_{cat}}\left(\frac{dX_A}{dt}\right)_{t=0}, \quad (1)$$

where r_{A0} is the initial rate of reaction, n_{A0} is the initial moles of reactant A, W_{cat} is the weight of catalyst, and X_A is the conversion of acetic acid at time t. The differential term in the above equation is the slope of the acetic acid conversion *vs* time curves shown in Fig. 2.

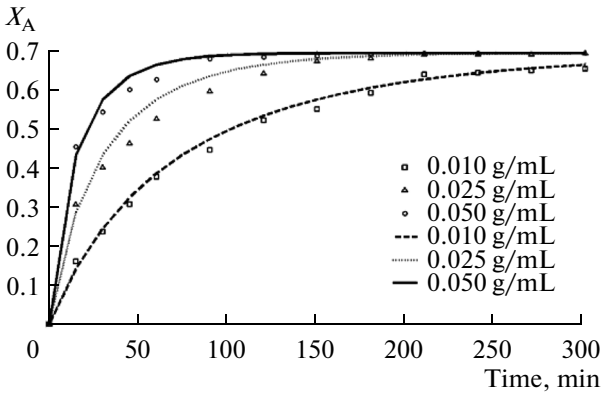

Fig. 2. Conversion acetic acid for different catalyst concentrations at 343.15 K. Dashed lines represents the LHHW model predictions.

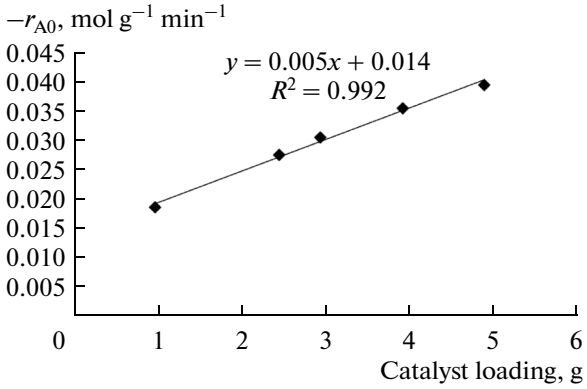

Fig. 3. Effect of catalyst loading on the initial reaction rate. Solid line represents the trend line fitting to the experimental data.

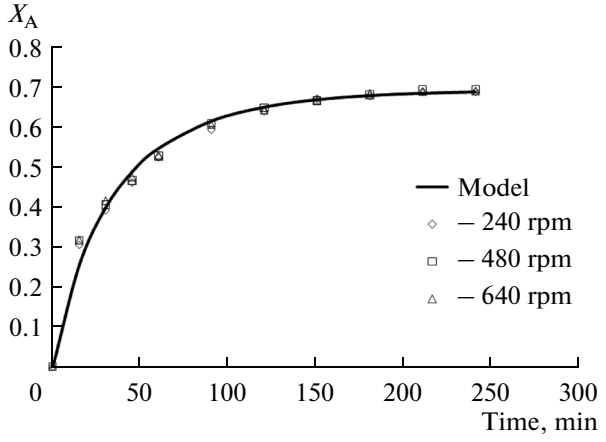

Fig. 4. Conversion of acetic acid at different agitation speeds. Solid line represents the LHHW model prediction.

The experimental data has been fitted to fifth order polynomial and slope is evaluated at time equal to zero.

$$X_A = c_0 + c_1 t + c_2 t^2 + c_3 t^3 + c_4 t^4 + c_5 t^5, \quad (2)$$

where $c_i = \text{const}$, $i = 0–5$.

Figure 3 shows the initial reaction rate as a function of the catalyst concentration. The plot shows a linear relationship between the initial reaction rate and catalyst concentration. Further the reaction rate increases as the catalyst loading increases. At higher catalyst concentrations the reaction reaches equilibrium faster. The mathematical equation relating to the initial reaction rate to the catalyst loading and obtained from Fig. 3 is given below.

$$-r_{A0} = 0.005 W_{cat} + 0.014, \quad (3)$$

where W_{cat} is the catalyst loading.

Effect of Stirring Rate

To study the effect of mass transfer resistance on the esterification reaction, experiments were conducted at the range of stirring rates from 240 to 640 rpm. Other experimental conditions are: molar ratio = 1 : 1, [catalyst] = 0.025 g/mL, T = 343.15 K, average catalyst particle size = 725 μm and Indion 190 as a catalyst. Figure 4 shows the kinetics of conversion of acetic acid at different stirring rates along with the expected values derived from the LHHW model. From this experimental data it can be deduced that the conversion of acetic acid is not affected by the stirrer rate. This indicates that the external mass transfer resistance is negligible for the esterification reaction and a minimum stirring rate of 240 rpm maintained for mixing catalyst in the reaction mixture. This finding is agreement with the results of Chakrabarti and Sharma [8], who established that the external mass transfer is not controlling the overall reaction rate, except for cases in which the stirring rate is very low or the viscosity of the reaction mixture is very high.

Effect of Catalyst Particle Size

To study the effect of catalyst particle size, experiments were conducted using catalysts with the average particle sizes of 425, 550, 725, and 925 μm. The Indion190 catalyst was screened to fractions with different particle sizes as given in Table 2. Figure 5 shows the effect of the average particle size for the same mass loading on the kinetics of acetic acid transformation. The figure is supplemented by the expected data derived from the LHHW model. Figure 5 indicates that the average catalyst particle size has no significant effect on the acetic acid conversion for the catalysts with given average sizes. The equilibrium conversion in all cases was reached in about 200 min. This further confirms that mass transfer limitation does not affect rates of esterification. Liu and Tan [21] pointed out that intra-particle diffusion resistances is usually neg-

ligible for most of the reactions catalyzed by the Amberlyst type catalysts. The present results are in good agreement with literature results [22–26].

Effect of Initial Reactant Molar Ratio

The initial molar ratio of acetic acid to methanol was varied from 1 : 1 to 1 : 4. The other experimental conditions maintained were: Indion 190 as a catalyst, [catalyst] = 0.025 g/mL, T = 343.15 K and stirrer rate = 240 rpm. Figure 6 shows the effect of initial molar ratio on acetic acid conversion. The figure shows that the equilibrium conversion of acetic acid increases with increase in molar ratio caused by the excess methanol. When the molar ratio of acetic acid to methanol was increased from 1 : 1 to 1 : 4, the equilibrium conversion of acetic acid increased from 68.5 to 92.4%.

KINETIC MODEL

The experimental data is correlated with the different kinetic models. The kinetics models are described in the following sections.

Pseudo-homogeneous Model

Most of the ion-exchange resins catalysed reactions are classified as pseudo-homogeneous. The system can be assumed as ideal if the catalyst is completely swelling or SO_3H groups of the polymer catalyst are completely dissolved in the solution [8]. A pseudo-homogeneous model can be applied for the reactions with a negligible mass transfer resistance and with a highly polar reactant or product [8]. The pseudo-homogeneous model is based on the Helfferich approach, in which the catalysis by ion-exchange resin assumed to be in homogeneous phase, whereas the reactants and products within in catalyst mass are in equilibrium with the bulk solution. The swelling of the catalyst in the presence of polar solvent like water leads to easy accessibility of the acid groups for the reaction and easy transport of the reactants and products. In the present system, water forms as a product. Accordingly, it can improve the swelling of the ion-exchange resin catalyst in the course of the reaction [27].

Table 2. Indion190 particle size distribution

Particle diameter size, μm	Weight fraction, ×100%
>1000	0.28
850–1000	49.65
600–850	15.54
500–600	29.11
350–500	4.90
<350	0.28

The pseudo-homogeneous kinetic equation for the reversible esterification reaction is given below

$$-r_i = \frac{1}{\nu_i}\frac{1}{m_{\text{cat}}}\frac{\mathrm{d}n_i}{\mathrm{d}t} = k_{\text{f}}a_{\text{A}}a_{\text{B}} - k_{\text{b}}a_{\text{C}}a_{\text{D}} = k_{\text{f}}\left(a_{\text{A}}a_{\text{B}} - \frac{a_{\text{C}}a_{\text{D}}}{K_{\text{eq}}}\right), \quad (4)$$

$$K_{\text{eq}} = \frac{k_{\text{f}}}{k_{\text{b}}} = \frac{x_{\text{C}}^{\text{eq}}x_{\text{D}}^{\text{eq}}\gamma_{\text{C}}^{\text{eq}}\gamma_{\text{D}}^{\text{eq}}}{x_{\text{A}}^{\text{eq}}x_{\text{B}}^{\text{eq}}\gamma_{\text{A}}^{\text{eq}}\gamma_{\text{B}}^{\text{eq}}}. \quad (5)$$

The stoichiometric coefficient $\nu_i = 1$ for all the components. The system behaves as ideal if $\gamma_i = 1$ for all the components. The non-ideality of the liquid phase reaction is taken into account by using the activities instead of mole fractions in Eq. (4). The activity coefficients were calculated by using the UNIQUAC model [28]. The UNIQUAC parameters related to van der Waals volume (r_i), surface values (q_i) and temperature dependent interaction parameters were taken

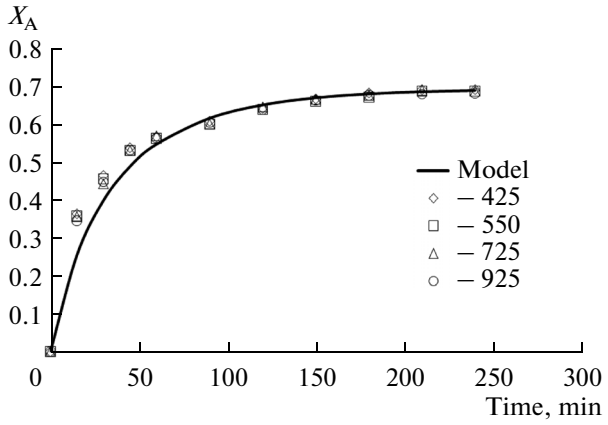

Fig. 5. The effect of the catalyst particle size (in μm) on the conversion of acetic acid. Solid line represents the LHHW model prediction.

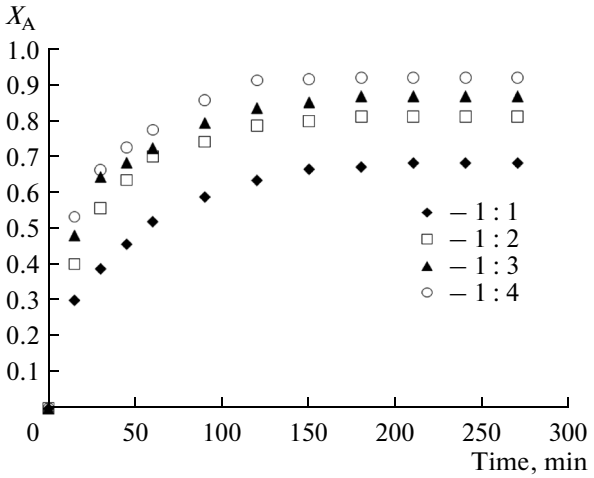

Fig. 6. The effect of the acetic acid to methanol molar ratio on acetic acid conversion.

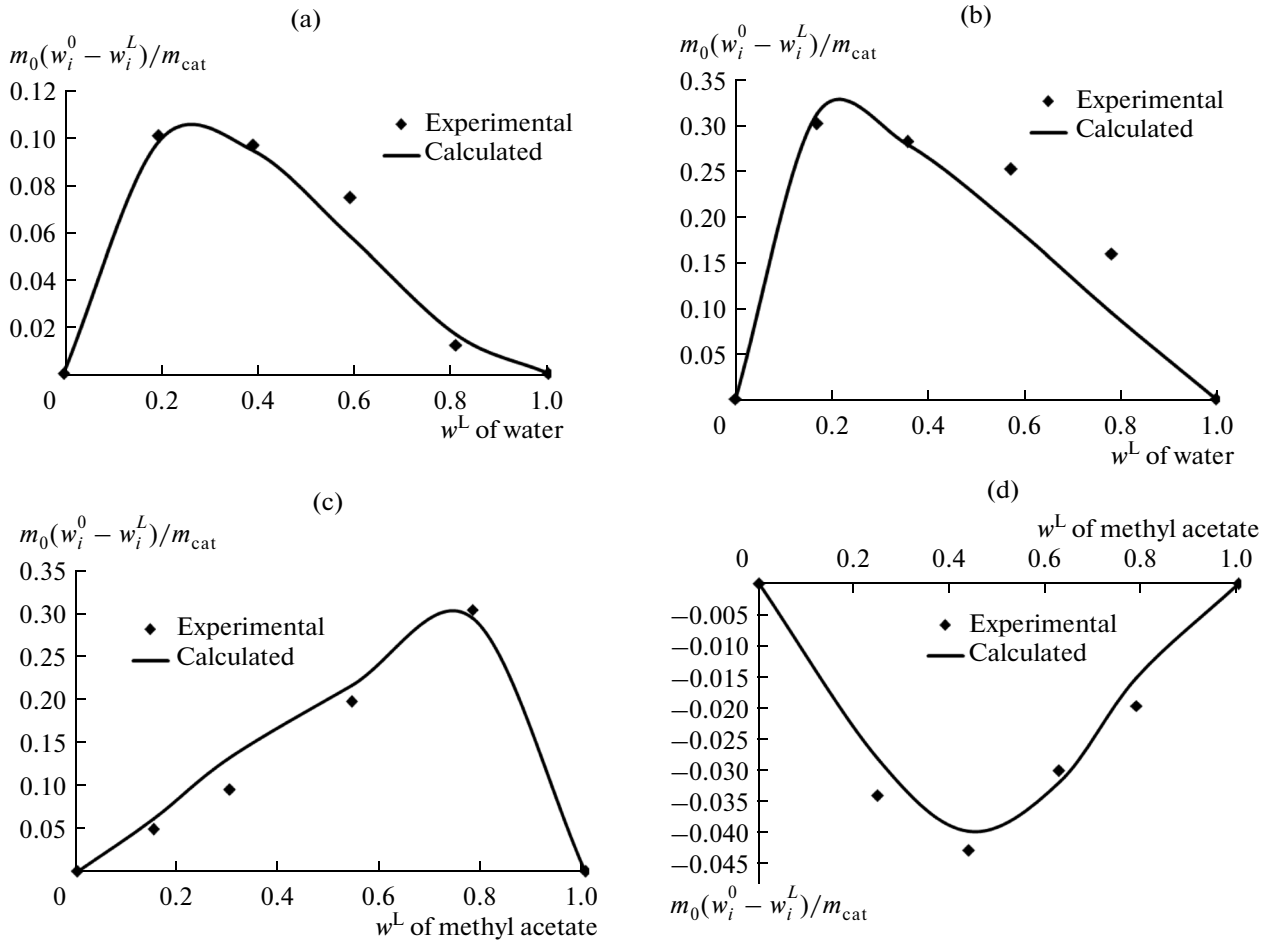

Fig. 7. Results of adsorption experiments for nonreactive binary systems of the relative adsorption of water from water-methanol (a) and water-acetic acid (b), the relative adsorption of methyl acetate from methyl acetate-methanol (c) and methyl acetate-acetic acid (d) at 298.15 K temperature.

from literature [29]. The effect of temperature on the reaction rate constants is expressed by the Arrhenius equation

$$k_f = k_{f0} \exp\left(-\frac{E_f}{RT}\right), \quad (6)$$

$$k_b = k_{b0} \exp\left(-\frac{E_b}{RT}\right), \quad (7)$$

where k_{f0} and k_{b0} are pre-exponential factors of forward and backward reactions (in mol g^{-1} min^{-1}), E_f and E_b are the activation energies of forward and backward reactions (in J/mol), R is the gas constant and T is temperature (in K).

The kinetic rate equation is integrated by using Runge–Kutta 4th order method using ode45 Matlab program. The kinetic parameters were fitted to the experimental data by minimizing the mean squared deviation between the experimental and calculated conversions of acetic acid. Four adjustable parameters, frequency factors (k_{f0} and k_{b0}) and activation energies (E_f and E_b) were fitted to the pseudo-homogeneous kinetic equation.

The calculated conversions of the acetic acid compared with the experimental values to find the mean relative error (F_{rel}) and the mean squared deviation (F_{abs}) are given below. The maximum allowable error to find the constants was 5%.

$$F_{rel} = \frac{\sum^{n_s} \left| \frac{X_{A,exp} - X_{A,cal}}{X_{A,cal}} \right|}{n_s}, \quad (8)$$

$$F_{abs} = \frac{\sum^{n_s} \left(X_{A,exp} - X_{A,cal}\right)^2}{n_s}, \quad (9)$$

where n_s is total data points.

Adsorption Based Models

There are two adsorption based models viz Eley–Rideal (ER) and Langmuir–Hinshelwood–Hougen–Watson (LHHW) models. ER and LHHW models are often used when adsorption effects play a significant

Table 3. Experimental data for swelling ratios, adsorbed volumes, masses and moles per gram of dry catalyst for the pure components at 298.15 K

Component	Swelling ratio	Adsorbed volume, cm^3/g	Adsorbed mass, g/g_{cat}	Adsorbed amount, $mmol/g_{cat}$
Acetic acid	1.33	0.2645	0.328	5.40
Methanol	1.36	0.2572	0.319	9.90
Methyl acetate	1.28	0.2200	0.273	3.68
Water	1.45	0.4030	0.480	26.70

role in the reaction. In adsorption based models it is assumed that the process is controlled by the reaction on the catalyst surface. LHHW model assumes that the reaction predominantly occurs between two reactant molecules adsorbed on the catalyst surface. On the other hand, the ER model assumes that only one of the reactant molecules adsorbs and another one reacts with it without adsorbing.

The adsorption based kinetic model equations are described below.

$$\text{ER model: } -r_i = \frac{1}{v_i}\frac{1}{m_{cat}}\frac{dn_i}{dt} = \frac{k_f a_A a_B - k_b a_C a_D}{\left(1 + \sum_{i=1}^{n} K_i a_i\right)}, \quad (10)$$

$$\text{LHHW model: } -r_i = \frac{1}{v_i}\frac{1}{m_{cat}}\frac{dn_i}{dt} = \frac{k_f a_A a_B - k_b a_C a_D}{\left(1 + \sum_{i=1}^{n} K_i a_i\right)^2}, \quad (11)$$

where a_i is activity of component i ($a_i = \gamma_i x_i$) and K_i is the adsorption constant of pure component i. The adsorption constant is defined as the ratio between the concentrations of the component in solid phase (in catalyst) and in the solution.

The adsorption constants were taken as adjustable parameters in Eq. (12) by fitting adsorption data obtained from binary nonreactive mixture adsorption experiments, as described in the experimental section. In addition m^s/m_{cat} was also taken adjustable parameter in Eq. (12). In this esterification reaction, the 4 nonreactive binary systems (methyl acetate–methanol, methyl acetate–acetic acid, water–methanol and water–acetic acid) were investigated. The sorption results are shown in Fig. 7. The adsorption constants were obtained for the nonreactive binary system by assuming Langmuir type (L) adsorption proposed by Popken et al. [12]:

$$\frac{m_0\left(w_i^0 - w_i^L\right)}{m_{cat}} = \frac{m^s}{m_{cat}}\frac{K_i a_i w_j^L - K_j a_j w_i^L}{\left(1 + K_i a_i + K_j a_j\right)}, \quad (12)$$

where m_0 is mass of liquid mixtures, m_{cat} is the mass of the catalyst, w_i^0 is the initial weight fraction of component i, w_i^L and w_j^L is the equilibrium weight fraction of component i and component j, K_i and K_j are the adsorption constants of component i and component j and m^s/m_{cat} is the total amount of adsorbed mass per unit mass of catalyst. In this equation values of i and j vary from 1 to 4.

The swelling experimental results are shown in Table 3. The swelling ratio is the ratio of volume of resin catalyst at equilibrium with pure components to the volume of the dry catalyst. When the quantity adsorbed is given as the weight in grams per gram of the catalyst rather than in moles, it can be deduced from Table 3 that the amount of adsorbed species on the catalyst is nearly constant for all four components (i.e. for methanol 0.319 g/g based on mass and 9.9 mmol/g based on moles). The adsorption constants and adsorbed mass of solvents were fitted to the binary sorption data by minimizing the error between the experimental results and model data with accuracy of ±5% error and the results are presented in Table 4. For calculation of adsorption constants mass relations were used. The values of adsorption constants given as mol/g of the catalyst decrease in the order water > methanol > acetic acid > methyl acetate in agreement with the results reported in literature [12].

The parameters obtained from the experimental data with different kinetic models are listed in Table 5. High values of activation energies in Table 5 are consistent with the idea that the reaction takes place only on the catalyst surface and it is not diffusion controlled [30]. The results described in the experimental section suggest that neither stirring rate nor the size of the catalyst particle significantly affect the acetic acid conversion indicating a negligible role of the internal and external mass transfer limitations. From Table 5 it can be recognized that all the kinetic models fit experi-

Table 4. Results of nonreactive binary adsorption equilibrium on Indion 190 catalyst at 298.15 K (Eq. 12)

m^s/m_{cat}	Adsorption constants, mol/g			
	acetic acid, K_1	methanol, K_2	methyl acetate, K_3	water, K_4
0.85	2.83	5.9	3.0	5.5

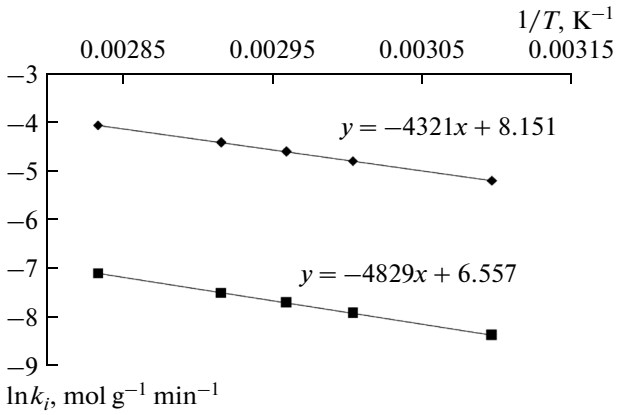

Fig. 8. Arrhenius diagram used to evaluate reaction rate constants for the forward and backward reactions. Solid line represents the trend line fitting to the data.

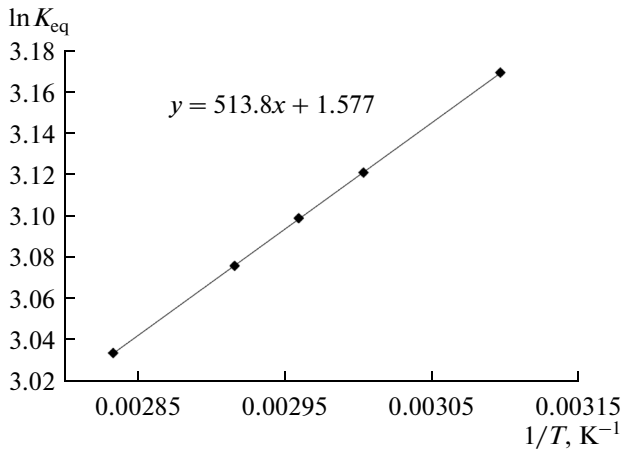

Fig. 9. Temperature dependence of the equilibrium constant. Solid line represents the trend line fitting to the data.

mental results fairly good. But among the kinetic models considered, but with the LHHW model a more accurate match of the experimental data was achieved.

The influence of temperature on the reaction rate for LHHW model is determined by fitting k_f and k_b to the Arrhenius equation. Figure 8 shows Arrhenius diagram for the relationship between the forward and backward reaction rate constants. It can be inferred from the plot that at a fixed catalyst concentration the reaction rate constants increase with temperature. The activation energies for both the forward and backward reactions are found to be 35.9 ± 0.5 and 40.2 ± 0.6 kJ/mol, respectively.

The heat of a reaction was calculated from Van't Hoff's equation

$$\ln K_{eq} = \left(\frac{-\Delta H_r^0}{RT}\right) + \left(\frac{\Delta S^0}{R}\right). \quad (13)$$

Van't Hoff's equation provides information about the temperature dependence of the equilibrium constant. From Fig. 9, the slope of the $\ln K_{eq}$ versus $1/T$ was calculated and from that slope the heat of reaction was evaluated. The heat of reaction for the present reaction is -4.27 ± 0.06 kJ/mol. This value, closed to the value calculated from the standard enthalpy of formation, indicates the exothermic pattern of the reaction [31, 32].

CONCLUSIONS

The experimental data outlined above indicate that the esterification reaction between the acetic acid and methanol is kinetically controlled rather than mass transfer limited. The kinetic parameters were found for different kinetic models, pseudo-homogeneous (ideal and non-ideal), Eley–Rideal (ER) and Langmuir–Hinshelwood–Hougen–Watson (LHHW). All the kinetic models were able to predict the experimental data equally well within the error of less than 5%. Compared to other models with the LHHW model a more accurate match of the experimental data was achieved. Temperature dependency of equilibrium constant on the reaction was calculated from Van't Hoff's equation. Based on the LHHW model the heat

Table 5. Adjustable parameters and residual errors of the different kinetic models to fit the experimental data with model predictions for Indion 190 as catalyst

Model	k_{f0}	k_{b0}	E_f	E_b	ΔH_r	ΔS, J/mol	Mean relative error F_{rel}, %	Mean squared deviation F_{abs}
	mol g^{-1} min^{-1}		kJ/mol					
Pseudo-homogeneous (UNIQUAC)	3479	715	35.9 ± 0.5	40.2 ± 0.6	-4.27 ± 0.06	13.1 ± 0.2	4.95	7.9×10^{-4}
Pseudo-homogeneous (ideal)	3829	1153	36.5 ± 0.3	37.8 ± 0.3	-1.47 ± 0.01	9.9 ± 0.1	5.85	8.9×10^{-4}
ER model	4000	840	36.0 ± 0.2	40.2 ± 0.3	-4.26 ± 0.03	12.9 ± 0.1	4.45	7.1×10^{-4}
LHHW model	4210	930	35.6 ± 0.3	39.9 ± 0.4	-4.59 ± 0.04	11.9 ± 0.1	2.91	4.0×10^{-4}

of reaction was found to be -4.27 ± 0.06 kJ/mol with Indion 190 as a catalyst.

NOTATION

a—activity
c_i—constant ($i = 0$ to 5)
E_f—activation energy of the forward reaction (J/mol)
E_b—activation energy of the backward reaction (J/mol)
ΔH_r—heat of reaction (J/mol)
K_{eq}—equilibrium constant
k_f—rate constant of the forward reaction (mol $g^{-1}min^{-1}$)
k_b—rate constant of the backward reaction (mol $g^{-1}min^{-1}$)
k_{f0}—frequency factor of the forward reaction (mol $g^{-1}min^{-1}$)
k_{b0}—frequency factor of the backward reaction (mol $g^{-1}min^{-1}$)
n_{A0}—initial mole numbers of acetic acid (mol)
n_s—total data points
r_A—reaction rate of acetic acid (mol $g^{-1}min^{-1}$)
R—gas constant (J mol^{-1} K^{-1})
T—absolute temperature (K)
t—time (min)
W_{cat}—catalyst loading (g)
X_A—acetic acid conversion
x—mole fraction
γ—activity coefficient

REFERENCES

1. Yadav, G.D. and Mehta, P.H., *Ind. Eng. Chem. Res.*, 1994, vol. 33, p. 2198.
2. Peters, T.A., Benes, N.E., Holmen, A., and Keurentjes, J.T.F., *Appl. Catal., A*, 2004, vol. 297, p. 182.
3. Rolfe, C. and Hinshelwood, C.N., *Trans. Faraday Soc.*, 1934, vol. 30, p. 935.
4. Ronnback, R., Salmi, T., Vuori, A., Haario, H., Lehtonen, J., Sundqvist, A., and Tirronen, E., *Chem. Eng. Sci.*, 1997, vol. 52, p. 3369.
5. Agreda, V.H., Partin, L.R., and Heiss, W.H., *Chem. Eng. Process.*, 1990, vol. 86, no. 2, p. 40.
6. Yadav, G.D. and Thathagar, M.B., *React. Funct. Polym.*, 2002, vol. 52, p. 99.
7. Zhang, Y., Ma, L., and Yang, J., *React. Funct. Polym.*, 2004, vol. 61, p. 101.
8. Chakrabarti, A. and Sharma, M.M., *React. Funct. Polym.*, 1993, vol. 20, p. 1.
9. Altiokka, M.R. and Citak, A., *Appl. Catal., A*, 2003, vol. 239, p. 141.
10. Pham, A.S., Shun, N., and Kohki, E., *React. Kinet. Mech. Catal.*, 2012, vol. 106, p. 185.
11. Yadav, G.D. and Kulkarni, H.B., *React. Funct. Polym.*, 2000, vol. 44, p. 153.
12. Popken, T., Gotze, L., and Gmehling, J., *Ind. Eng. Chem. Res.*, 2000, vol. 39, p. 2601.
13. Yu, W., Hidajat, K., and Ray, A.K., *Appl. Catal., A*, 2004, vol. 260, p. 191.
14. Kirbasla, S.I., Terzioglu, H.Z., and Dramur, U., *Chin. J. Chem. Eng.*, 2001, vol. 9, p. 90.
15. Winkler, E.B. and Gmehling, J., *Ind. Eng. Chem. Res.*, 2006, vol. 45, p. 6648.
16. Venkateswar Rao, T., Sapna, B., Priyanka, B., Chandrashekar, P., and Jagadish, K., *Reac. Kinet. Mech. Catal.*, 2009, vol. 107, p. 449.
17. Erdem, B. and Cebe, M., *Korean J. Chem. Eng*, 2006, vol. 23, no. 6, p. 896.
18. Song, W., Venimadhavan, G., Manning, J.M., Malone, M.F., and Doherty, M.F., *Ind. Eng. Chem. Res.*, 1998, vol. 37, p. 1917.
19. Liu, Y., Lotero, E., and Goodwin, J.G., *J. Catal.*, 2006, vol. 242, p. 278.
20. Tsai, Y.T., Lin, H.M., and Lee, M.J., *Chem. Eng. J.*, 2011, vol. 171, p. 1367.
21. Liu, W.T. and Tan, Ch.S., *Ind. Eng. Chem. Res.*, 2011, vol. 40, p. 7155.
22. Titus, M.P., Bausach, M., Tejero, J., Ibarra, M., Fite, C., Cunill, F., and Izquierdo, J.F., *Appl. Catal., A*, 2007, vol. 323, p. 38.
23. Ali, S.H., Tarakmah, A., Merchant, S.Q., and Al-Sahhaf, T., *Chem. Eng. Sci.*, 2007, vol. 62, p. 3197.
24. Mao, W., Wang, X., Wang, H., Chang, H., Zhang, X., and Han, J., *J. Chem. Eng. Process.*, 2008, vol. 47, p. 761.
25. Delgado, P., San, M.T., and Beltran, S., *Chem. Eng. J.*, 2007, vol. 126, p. 111.
26. Cruz, V.J., Izquierdo, J.F., Cunill, F., Tejero, J., Iborra, M., Fite, C., and Bringue, R., *React. Funct. Polym.*, 2007, vol. 67, p. 210.
27. Helfferich, F., *Ion Exchange*, New York: McGraw-Hill, 1962.
28. Abrams, D.S. and Prausnitz, J.M., *AIChE J.*, 1975, vol. 21, p. 116.
29. Gmehling, J. and Onken, U., *DECHEMA Chemistry Data Series*, Frankfurt: DECHEMA, 1977, vol. 1, part 1.
30. Steinigeweg, S. and Gmehling, J., *Chem. Eng. Process.*, 2004, vol. 43, p. 447.
31. Barin, I., *Thermochemical Data of Pure Substances*, Weinheim: VCH, 1989.
32. Domalski, E.S. and Hearing, E.D., *J. Phys. Chem. Ref. Data*, 1993, vol. 22, p. 805.